

A finite element analysis modeling tool for solid oxide fuel cell development: coupled electrochemistry, thermal and flow analysis in MARC®

M.A. Khaleel^{a,*}, Z. Lin^a, P. Singh^a, W. Surdoval^b, D. Collin^b

^a Pacific Northwest National Engineering Mechanics Group Laboratory, P.O. Box 999, Mail Stop K2-18, Richland, WA 99352, USA

^b National Energy Technology Laboratory, Morgantown, WV 26507-0880, USA

Received 6 November 2003; accepted 29 November 2003

Abstract

A 3D simulation tool for modeling solid oxide fuel cells is described. The tool combines the versatility and efficiency of a commercial finite element analysis code, MARC®, with an in-house developed robust and flexible electrochemical (EC) module. Based upon characteristic parameters obtained experimentally and assigned by the user, the EC module calculates the current density distribution, heat generation, and fuel and oxidant species concentration, taking the temperature profile provided by MARC® and operating conditions such as the fuel and oxidant flow rate and the total stack output voltage or current as the input. MARC® performs flow and thermal analyses based on the initial and boundary thermal and flow conditions and the heat generation calculated by the EC module. The main coupling between MARC® and EC is for MARC® to supply the temperature field to EC and for EC to give the heat generation profile to MARC®. The loosely coupled, iterative scheme is advantageous in terms of memory requirement, numerical stability and computational efficiency. The coupling is iterated to self-consistency for a steady-state solution. Sample results for steady states as well as the startup process for stacks with different flow designs are presented to illustrate the modeling capability and numerical performance characteristic of the simulation tool. © 2004 Elsevier B.V. All rights reserved.

Keywords: Solid oxide fuel cell; Finite element method; Computer modeling; Electrochemical reaction; Thermal analysis; Flow model

1. Introduction

A solid oxide fuel cell (SOFC) is a device that converts chemical energy into electrical energy continuously by means of an electrochemical (EC) process. The high operating temperature of SOFCs has numerous advantages. For example, kinetic activity is high and nickel is a sufficiently good catalyst, eliminating the need to use costly precious metals. CO can be used as fuel instead of as a poison, as in other low temperature fuel cells, offering potential for fuel flexibility and high efficiency. Natural gas fuel can be reformed within the cell stack, eliminating the need for an expensive external reformer system. SOFCs also offer the possibility of heat co-generation for even higher efficiency. However, the high operating temperature can lead to complex materials problems, including mechanical stress due to the different thermal expansion coefficients of the cell components; electrode sintering, interfacial diffusion between electrolyte, electrode and interconnect materials. All these

factors decrease the efficiency and the stability of the cell. The choice of component materials is limited, and fabrication problems further increase the cost of manufacturing. SOFCs also require more time and energy for startup. Such problems have limited the commercial development of SOFCs.

Planar-type designs have received much attention recently because they potentially offer higher power density than the tubular-type SOFC. This is attributed to the low electrical resistance due to shorter current paths. In particular, a very thin electrolyte film can be used in an anode-supported SOFC, drastically reducing the Ohmic resistance and enabling operation at intermediate temperatures, maintaining this benefit while alleviating the associated material and mechanical difficulties.

Despite wide interest and intensive research as well as significant progress, current SOFCs represent an immature technology. To be commercially feasible, major development is required on: (1) lowering the cost of manufacture; (2) improving durability to match that of other electrical generation techniques in use; and (3) increasing efficiency to approach the theoretical limit, thus broadening the range

* Corresponding author. Tel.: +1-509-375-2438; fax: +1-509-375-6605.
E-mail address: moe.khaleel@pnl.gov (M.A. Khaleel).

of potential applications. This development requires examining a huge parameter space of potential operating temperatures, materials, plate and component designs, geometries, dimensions, optimization of stack configurations, fuels, reformers, heat exchangers, and others.

Although the design and operation of an SOFC appear deceptively simple, many of the phenomena dominating the performance of the SOFC are complex, competing, and not well understood. Experimental advances are limited because physical prototyping is expensive, time consuming, and cannot explore a range of designs and operating conditions. To speed up the development and understanding of SOFCs, it is highly desirable to establish mathematical models that incorporate the known physics and behavior of SOFC materials to predict and improve performance.

A mathematical simulation of an SOFC is helpful in examining various operating parameters such as temperatures, materials, geometries, dimensions, fuels, reformers, etc. and determining their associated performance characteristics. Such a simulation can be used to determine the effect of varying the design and operating parameters on the power generated, fuel conversion efficiency, maximum cell temperature reached, stresses caused by temperature gradients, and the effects of different coefficients of thermal expansion for the electrolyte, electrodes and interconnect. In addition, such simulations can provide answers to questions such as how much the electrical properties of the cell materials need to be improved or what the air and fuel flow rates must be to avoid excessive temperature and/or pressure drop. Thus, mathematical simulation offers the potential to direct the technology development, test the significance of various design features and effectiveness of developments in materials or fabrication procedures, and select optimum operating conditions from the feasible set of process parameters. Modeling of SOFCs is a critical aspect of the SOFC technology development process.

A key feature of the Core Technology program sponsored by the US Department of Energy is the development of modeling and simulation tools that are applicable to a wide range of SOFC designs and easily accessible to the SOFC research and development (R&D) community. As the constitutive thermal, chemical, EC, and transport processes are strongly coupled, the SOFC operations involve multi-physics processes and require versatile multi-physics tools for realistic descriptions. However, no available commercial code has the capability to treat the fully coupled physical processes involved in SOFCs. Though there are many model development efforts, most resulting proprietary software has significant limitations and/or not widely available. One exception is the software developed by Recknagle et al. [1] who created a SOFC modeling tool based on a commercial computational fluid dynamics (CFD) package, STAR-CD. However, the CFD algorithm of STAR-CD makes the numerical stability and computational efficiency less favorable. To assist the technology development that involves design optimization of various geometric, material

and operational parameters, parametric studies are often required. As the cost of such parametric studies increases exponentially with the number of working parameters, and many such parameters are involved in SOFC designs, the computational efficiency of the modeling tool is of critical importance in many regards and is highly desirable. To this end, a numerically stable and efficient algorithm is preferred.

As commercially available finite element (FE) codes are well developed and have a long history of successful application in structural design, commercial FE codes appear to be natural choices for the platform of the SOFC modeling tool. In particular, the MARC[®] FE code from MSC Software is a multi-physics, robust structural (mechanical, thermal, etc.) analysis tool. MARC[®] has a full library of user subroutines that allow for user interaction with the code. Its user-defined functions allow algorithms describing the chemical and EC processes and heat generation to be incorporated efficiently. Consequently, MARC[®] was selected as the underlying platform for integration with the in-house developed EC module, which models the EC, chemical reaction, and heat generation.

The goal of this paper is to describe the capability of our EC module and the coupling of our EC model with the MARC[®] FE analysis (FEA) code. The EC model determines the current distribution, gas species concentration, and heat generation, and the FE code solves the heat transfer problem. This tool will allow for a variety of designs, materials, geometries, and flow conditions to be evaluated at both transient and steady-state operating conditions.

Section 2 of this paper describes the theoretical background and associated technical details of the EC software module. The EC theory contains a detailed account of the chosen current–voltage (I – V) relations and associated heat production. Determination of the equilibrium contents of multi-component fuels is also described to treat fuels with CO and CH₄ and possibly other hydrocarbon fuels. The calculation of the heat production due to the chemical reactions is also described. Section 3 describes the overall algorithm and functionality of the EC module and the linkage between the EC module and the MARC[®] FEA code. Section 4 shows a prototype SOFC cell and stack model and the corresponding sample results. The numerical performance of the coupled MARC[®]–EC package is also described. A brief summary is given in Section 5.

2. Theoretical background and technical details

In a fuel cell operation, the flow, thermal, chemical, and EC systems are intrinsically coupled. The temperature and flow field determine the rate of chemical and EC reaction. Heat generation and absorption by the chemical and EC reactions in turn affect the temperature distribution and gas flow composition. The coupling requires an iterative procedure to achieve a self-consistent solution. MARC[®] performs the thermal analysis if all heat flux is properly accounted

for. The key linkage between the EC module and MARC[®] is for the EC module to feed MARC[®] with the heat flux resulting from the chemical and EC reactions, which are based on the temperature field MARC[®] provides the EC module. The description for the heat transfer solution is referred to in the MARC[®] documentation, and only the basic theory and implementation details relevant to the EC module are described here.

The EC process generates the electrical power needed for the SOFC applications. SOFC efficiency depends on optimization of plate design, stack configurations, and operating conditions as well as understanding the complex interactions between various EC phenomena. The EC and chemical processes generate heat, which results in thermal stresses and affects structural reliability. Consequently, the EC process is the heart of the fuel cell. One of the most important aspects of SOFC design is the voltage and current distribution in the cell plate. This couples with the temperature distribution from the thermal and flow model and also with the EC reactions at the electrodes.

Overall, the EC module gives the solutions to the current density distribution, species concentration, chemical reaction, heat generation, and flow field. The EC is treated at the effective property or continuum level, i.e., the simulation of electrode and cell performance involves some parameterized EC models. Such an EC model is described as a current–voltage relation, or I – V curve, for a single cell, in terms of parameters that are effective cell properties and operational parameters. The solutions to the chemical reactions (CO–water shift reaction, CH₄ internal reforming, etc) are based on the equilibrium theory. The flow solution is based on the approximation of a quasi-two-dimensional laminar flow (flow in each gas channel is treated as one-dimensional). Mass balances are used with the flow pattern to establish species concentrations and fluxes at any point in the fuel cell. Each aspect of the EC module is described below.

2.1. I – V model for H₂ fuel

In the EC module of the MARC[®]–EC package, the EC is based on continuum-level I – V relations. The I – V relation describes the voltage (potential) loss at a specified current with respect to the ideal thermodynamic performance, which is called overpotential or polarization. That is, the I – V relation is a model for calculating current density, cell voltage, and heat production in an SOFC cell with H₂ or other fuels, taking as inputs local values of the gas partial pressures and temperatures. This cell I – V curve is specific for the materials, structural characteristics, and operational parameters (gas compositions, pressure, temperature) of a given PEN (cathode–electrolyte–anode) element. The user can change the relevant parameters to reflect their cell's EC performance.

Two I – V formulas and the associated parameters are implemented in the EC module. In this section, we describe in detail the I – V relation that fits best with H₂ fuel, though, as

discussed later, it can also be used for composite fuel without modification in most cases. Implementation details are also discussed. Generally, the I – V relation can be written as [2]:

$$V(i) = E_{\text{open}} - iRi - b \sinh^{-1} \left(\frac{i}{2i_0} \right) + C \ln \left(\frac{1-i}{i_{\text{O}_2}} \right) + 2C \ln \left(\frac{1-i}{i_{\text{H}_2}} \right) - 2C \ln \left(\frac{1+p_{\text{H}_2}^0 i}{p_{\text{H}_2\text{O}}^0 i_{\text{H}_2}} \right) \quad (1a)$$

Here, $C = RT/4F$, R is the gas constant, T the temperature, and F (96487 Coulomb/mol) the Faraday constant. In Eq. (1a), E_{open} is the equilibrium (open circuit) voltage, or emf (electromotive force), of the cell, i the current density, iRi the Ohmic potential drop, and i_0 the exchange current density; $b \sinh^{-1}(i/2i_0)$ represents the electrode activation polarization, i_{O_2} the O₂ transport limiting current, i_{H_2} the H₂ transport limiting current, $p_{\text{H}_2}^0$ the H₂ partial pressure, and $p_{\text{H}_2\text{O}}^0$ the H₂O partial pressure at the fuel channel. The last three terms represent, respectively, the O₂, H₂ and H₂O concentration polarization. Notice that $b \sinh^{-1}(i/2i_0)$ reduces to the familiar Tafel form for $i \gg i_0$, $b \ln(i/i_0)$, while eliminating its logarithmic divergence at $i = 0$. All the parameters in Eq. (1a) have clear physical meanings and their dependencies on the temperature, cell geometry, and gas partial pressures are known by experimental data and transport theory. In the following, the theory and the evaluation detail of each quantity that is necessary for software implementation are described.

The thermodynamic cell potential, or the Nernst potential, E_{open} , depends on reactant and product partial pressures as well as temperature. For example, for fuel with hydrogen only,

$$E_{\text{open}} = \frac{-\Delta G}{2F} \quad (2)$$

ΔG is the free energy change of the reaction $\text{H}_2 + 1/2\text{O}_2 \rightarrow \text{H}_2\text{O}$:

$$\Delta G = G_3 - G_1 - \frac{1}{2}G_2 \quad (3)$$

where G is the free energy per mole molecules. Subscript 1–3 refer to H₂, O₂, and H₂O, respectively.

The pressure and temperature dependence of the Nernst potential can be determined according to the thermodynamics. As ideal gas is a good approximation for the species involved in the operating condition, the pressure dependence of the Nernst potential can be written as:

$$E_{\text{open}} = - \left(\frac{\Delta G_{P_0}}{2F} \right) + \left(\frac{RT_1}{2F} \right) \ln p_1 + \left(\frac{RT_2}{4F} \right) \ln p_2 - \left(\frac{RT_1}{2F} \right) \ln p_3 \quad (4)$$

ΔG_{P_0} is the free energy change when all of the species are at $P_0 = 1$ atm and is, therefore, called the standard cell potential or standard emf. It depends only on temperature. T_1 and T_2 are the fuel and oxidant temperature, respectively.

Using the approximation $C_P = a + bT + cT^2$, which is found to fit the experimental data of many gases to within 0.5% over T from 0 to 1250 °C [3], the temperature dependence of the standard free energy can be calculated as:

$$G(T, P_0) = G(T_0, P_0) + a(T - T_0) + \frac{b}{2}(T^2 - T_0^2) + \frac{c}{3}(T^3 - T_0^3) - [TS(T, P_0) - T_0S(T_0, P_0)] \quad (5)$$

where

$$S(T, P_0) = S(T_0, P_0) + a \ln \frac{T}{T_0} + b(T - T_0) + \frac{c}{2}(T^2 - T_0^2) \quad (6)$$

and a , b , c , $S(T_0, P_0)$, and $\Delta G(T_0, P_0)$ are experimental data [3].

The electrical resistance, R_i , of the PEN structure is calculated simply as the sum of the cathode, R_p , electrolyte, R_e , anode, R_n , and bipolar, R_b , electrical resistances:

$$R_i = R_p + R_e + R_n + R_b \quad (7)$$

The ionic resistance of electrolyte is calculated as [4]:

$$R_e = l_e c_e T \exp\left(\frac{Q_e}{T}\right) \quad (8)$$

where l_e is the thickness of the electrolyte and Q_e the effective activation energy. R_p , R_n , and R_b are assumed to be Ohmic and have linear dependence on the temperature. The temperature dependence of the electrical resistance can also be defined by the user if desired.

For the thin cell structure we are interested in, $R_p + R_n + R_b$ is much smaller than R_e and may be neglected in practice. However, these terms are explicitly calculated in the software so the tool can describe cells with thicker electrodes/interconnects or other materials with some desirable properties but lower conductivity.

Notice that there are many other factors of practical importance not considered above. These include: (a) contact resistance: this depends on manufacturing process and can very well be more than the above resistance; (b) rib dimension: as channels increase the resistance of interconnect; (c) formation of highly resistive interfacial products such as $\text{La}_2\text{Zr}_2\text{O}_7$ and SrZrO_3 during cell operation and the electrode adhesion period [5]. One can add such data, if desired, in computing parameters such as resistance, current distribution, and heat generation.

Generally, the electrode activation polarization, $b \sinh^{-1}(i/2i_0)$, is strongly temperature dependent. The electrode activation polarizations are controlled by the reaction kinetics of the respective electrodes. They represent the voltage loss incurred due to the activation necessary for charge transfer and are usually dominated by the cathode process. One implementation in the package is to describe the temperature dependence by interpolation and extrapolation based on the available experimental data at several temperatures

provided in [2]. Notice that these data are cell dependent, and corresponding experimental data should be used in realistic simulations. Another implementation is to express the activation polarization in a Butler–Volmer form, i.e., writing $b = RT/\alpha F$, where α is the Butler–Volmer transfer coefficient. The exchange current density corresponds to the dynamic electron transfer rate at equilibrium, which is thermally activated. Therefore, the exchange current density can be expressed as [6]:

$$i_0 = P_x \exp\left(\frac{-E_{\text{act}}}{RT}\right) \quad (9)$$

where the prefactor, P_x , and the activation energy, E_{act} , are properties specific for the electrode–electrolyte interface in question.

Regarding the concentration polarization, the H_2 limiting current density is calculated as:

$$i_{\text{H}_2} = \frac{2FD_{\text{eff}}(T)p_{\text{H}_2}^0}{(RTl_a)} \quad (10)$$

where $D_{\text{eff}}(T)$ is the effective H_2 diffusion coefficient, $p_{\text{H}_2}^0$ the H_2 partial pressure, and l_a the anode thickness. In one option, the temperature-dependent portion of the expression is found by interpolation and extrapolation of the experimental data. Another option is to determine the temperature dependence according to the transport theory (described in more detail in Section 2.2). A similar method is used to find the O_2 limiting current density, though it is usually inconsequential for an anode-supported cell.

2.2. I - V model for fuel with CO

The anode concentration polarization terms of Eq. (1a) imply that all current is produced by H_2 oxidation. For fuel with CO, the measured current is the sum of the currents derived by H_2 (i_1) and CO (i_2) oxidation. Accordingly, the current for the anode concentration polarization terms in Eq. (1a) should be replaced with i_1 . Similar adjustment also applies to the current generated by CO oxidation. More specifically, Eq. (1a) should be changed to:

$$\begin{aligned} V(i) &= E_{\text{open}} - iR_i - b \sinh^{-1}\left(\frac{i}{2i_0}\right) + C \ln\left(\frac{1-i}{i_{\text{O}_2}}\right) \\ &\quad + 2C \ln\left(\frac{1-i_1}{i_{\text{H}_2}}\right) - 2C \ln\left(\frac{1+i_1}{i_{\text{H}_2\text{O}}}\right) \\ &= E_{\text{open}} - iR_i - b' \sinh^{-1}\left(\frac{i}{2i_0}\right) + C \ln\left(\frac{1-i}{i_{\text{O}_2}}\right) \\ &\quad + 2C \ln\left(\frac{1-i_2}{i_{\text{CO}}}\right) - 2C \ln\left(\frac{1+i_2}{i_{\text{CO}_2}}\right) \end{aligned} \quad (1b)$$

where $i_{\text{H}_2\text{O}} = p_{\text{H}_2\text{O}}^0 i_{\text{H}_2} / p_{\text{H}_2}^0$ is the limiting current for H_2O transport, i_{CO} and $i_{\text{CO}_2} = p_{\text{CO}_2}^0 i_{\text{CO}} / p_{\text{CO}}^0$ are, respectively, the limiting current for CO and CO_2 transport; b' is used to indicate the possible difference on the effective activation

polarization due to the CO current path. Generally speaking, CO is used in two ways, one by oxidation and produces current, the other by shift reaction and produces H₂. If the current is produced largely by CO oxidation, a reverse shift reaction could occur and H₂ (and CO₂) could be converted to CO (and H₂O). On the other hand, if the current is produced largely by H₂ oxidation, shift reaction would compensate for the depleted H₂. Though the same amount of current would generate a similar amount of heat and resulting similar gas composition by the two processes, the latter scenario is more likely as shift reaction is energetically favorable (9.84 kcal/mol). In fact, it is estimated that about 98% of current is produced by H₂ oxidation in common situations [7]. This implies that Eq. (1a) can also be used for CO fuel with minimal error. That is, we can often assume current is produced only by H₂ oxidation.

CO is shifted by the equilibrium condition. Parameters used for H₂ fuel can also be used here without modification (though one should bear in mind that it would be very different if CO is responsible for most of the current). This simplification is adopted in the software as one option. Another option is to explicitly consider the current produced by CO oxidation. The total current by the simultaneous H₂ and CO oxidation is treated by a parallel electrical circuit analogy [6]. Assuming the anode activation overpotential is negligible compared to the cathode activation polarization, or if the activation overpotential for H₂ and CO oxidation is the same, and the shift reaction does not proceed before the oxidation reaction, the diffusive polarization should be the same for H₂–H₂O and CO–CO₂ transport:

$$\begin{aligned} -\eta_{ac} &= 2C \ln \left(\frac{1 - i_1}{i_{H_2}} \right) - 2C \ln \left(\frac{1 + i_1}{i_{H_2O}} \right) \\ &= 2C \ln \left(\frac{1 - i_2}{i_{CO}} \right) - 2C \ln \left(\frac{1 + i_2}{i_{CO_2}} \right) \end{aligned} \quad (11)$$

With some algebra, the solution to Eq. (11) with a given total current yields:

$$t = \exp \left(\frac{-\eta_{ac}}{2C} \right) = \frac{-B + (B^2 - 4AC)^{1/2}}{2A} \quad (12)$$

where

$$A = \frac{i}{i_{H_2O} i_{CO_2}} + \frac{1}{i_{H_2O}} + \frac{1}{i_{CO_2}} \quad (13a)$$

$$B = \frac{i}{i_{H_2O} i_{CO}} + \frac{i}{i_{H_2} i_{CO_2}} + \frac{1}{i_{H_2}} + \frac{1}{i_{CO}} - \frac{1}{i_{H_2O}} - \frac{1}{i_{CO_2}} \quad (13b)$$

$$C = \frac{i}{i_{H_2} i_{CO}} - \frac{1}{i_{H_2}} - \frac{1}{i_{CO}} \quad (13c)$$

The current components are given by:

$$i_1 = \frac{1 - t}{(1/i_{H_2}) + (t/i_{H_2O})} \quad (14a)$$

$$i_2 = \frac{1 - t}{(1/i_{CO}) + (t/i_{CO_2})} \quad (14b)$$

These equations give the I – V relation when CO is present in the fuel stream. To complete the description for the limiting current as indicated by Eq. (10), one needs to determine the effective diffusion coefficients entering into the limiting currents for each gas species in the anode.

Diffusion coefficients for binary gas mixtures are fairly well known and scale fairly well with the result of elementary kinetic theory:

$$D \propto \frac{T^{3/2} (M_1^{-1} + M_2^{-1})^{1/2}}{p\sigma} \quad (15a)$$

where $T^{1/2}$ is the reduced mass reflect a rms thermal speed, a factor T/p comes from the density, and σ a scattering cross-section. We use a similar formula due to Fuller et al. [8] that incorporates a weak T -dependence of the cross-section:

$$D_{ij} = \frac{10^{-7} T^{1.75} (M_1^{-1} + M_2^{-1})^{1/2}}{p(r_i + r_j)^2} \quad (15b)$$

where D is in m²/s, T in Kelvin, the molecular weights are in amu, the pressure is in atmospheres, and the r 's are tabulated phenomenological molecular radii in arbitrary units. Data from [8] are used.

The full theory for a multinary gas mixture involves a diffusion matrix with off-diagonal elements in which the gradient of one component drives part of the current of the others. In addition to the mathematical complexity, the off-diagonal matrix elements are not well known. As an alternative, we compute a “unitary” diffusion coefficient for each species based on its binary coefficient with each of the others. As it is scattering rates or inverse conductivities that tend to be additive in such situations, a reciprocal average weighted by the fractional concentration y_i of each gas constituent is used:

$$(D_i)^{-1} = \sum_j y_j (D_{ij})^{-1} \quad (16)$$

The binary coefficients in Eq. (15) should be replaced with the unitary coefficients in Eq. (16) for the limiting current calculations. In the limit of an arbitrary binary mixture, Eq. (16) gives the exact result. It also approaches a ternary mixture correctly when one constituent is very dilute. With these formulae, the anode concentration polarization can be calculated for any given current and the I – V relation is determined.

2.3. Model for composite fuel: chemical equilibrium

Though most tests done for SOFC are done with H₂ fuel, fuel with CO, CH₄, or other hydrocarbon may be desirable in practice. The ability to treat fuels other than H₂ is required for modeling flexibility. The effects of CO fuel on the I – V relation and the possible treatments have been described

above in detail. The explicit determination of the composition change of the fuel, however, is still required. Moreover, more discussions are needed for hydrocarbon fuel. The general model we used in the software is that the current is either purely produced by H₂ oxidation (see Section 2.1) or by both H₂ and CO oxidation (see Section 2.2). The hydrocarbon is used not by oxidation but by steam reforming. The assumption is valid in most cases, though there are some exceptions [9,10]. The fuel composition change is determined by assuming chemical equilibrium. The equilibrium theory does not address the dynamic issue, i.e., how fast a system achieves equilibrium, which is strongly material and process dependent. While CO shift reaction is a fast process and can be assumed always to be at equilibrium, the steam reforming reaction may be a slow process and may not have reached equilibrium in the fuel cell operation [11]. The degree of deviation from the equilibrium and the effect on the modeling results depends on the actual fuel cell operating characteristics. More general treatment will be implemented later. The description below discusses the details of determining the fuel equilibrium compositions in the EC module.

2.3.1. Fuel with CO

For a given initial partial pressure of the CO fuel, P_{H_2} , P_{H_2O} , P_{CO} , and P_{CO_2} , the determination of the resulting content requires four conditions. Since no nuclear reaction is involved, each of the total contents of H, C and O should remain constant. The initial condition provides three constraints on the resulting content:

$$P_H = 2(P_{H_2} + P_{H_2O}) = \text{constant} \quad (17a)$$

$$P_C = P_{CO} + P_{CO_2} = \text{constant} \quad (17b)$$

$$P_O = P_{CO} + 2P_{CO_2} + P_{H_2O} = \text{constant} \quad (17c)$$

Thus, the remaining three compositions can be easily found when one component is determined. The fourth condition is provided by the equilibrium of the CO water shift reaction:



Assuming the equilibrium partial pressure should be $P_{H_2}^e$, $P_{H_2O}^e$, P_{CO}^e , $P_{CO_2}^e$, we have:

$$K_P = \frac{P_{H_2}^e P_{CO_2}^e}{P_{H_2O}^e P_{CO}^e} = \exp\left(\frac{-\Delta G_0}{RT}\right) \quad (19)$$

where ΔG_0 is the free energy change of the shift reaction when all reactants and products are at $P = 1$ atm. After some algebra, one finds:

$$P_{H_2}^e = \frac{-b + \sqrt{b^2 - 4(1 - K_P)c}}{2(1 - K_P)} \quad (20)$$

where

$$b = P_{CO_2} - P_{H_2} + K_P[P_{CO} + 2P_{H_2} + P_{H_2O}] \quad (21a)$$

$$c = -[P_{H_2} + P_{H_2O}][P_{CO} + P_{H_2}]K_P \quad (21b)$$

As indicated by the simple analytical expression, the equilibrium content determination requires negligible extra computation time.

2.3.2. Equilibrium composition for fuel with CH₄

For fuel with CH₄, there are five undetermined compositions, H₂, CO, H₂O, CO₂, and CH₄. It requires one more constraint than that of CO fuel. This additional constraint is provided by the equilibrium constant of the CH₄ steam reforming reaction:



Unlike the case with CO fuel, it is difficult to derive simple analytical expressions for the equilibrium compositions in this case. However, it is easy to devise a numerical solution. The algorithm for determining the equilibrium compositions involves the following steps:

- (1) Initial estimate CH₄ content.
- (2) Providing a sensible H₂, CO, H₂O, CO₂ composition, obeying the total content of H, C and O as the input and get the resulting shift equilibrium compositions, as described in the last subsection.
- (3) Check to see whether the steam reforming equilibrium condition is satisfied within the desired accuracy. If not, go back to Step (1) until the equilibrium content is found.

The software implementation for these steps is quite simple, and the overall equilibrium content can be obtained easily.

2.4. Flow model

The full treatment of gas flow movements requires a rigorous CFD tool and is computationally demanding. Though startup and transient processes as well as variations in certain operating parameters may have a sizeable effect on the flow profiles, the effect on the overall EC performance of the cell is not expected to be of the same order. As we are primarily concerned with the thermal and EC properties, it is not necessary to solve the details of the flow. Instead, it is desirable to make a simplification such as assuming laminar flow to reduce the computation cost and allow quick estimates of certain flow properties that are influential on the thermal and EC performance. To this end, the most relevant data are the species concentration profile and flow velocity.

Given the current density profile and flow rate, the species concentration can be obtained by the mass balance and the boundary conditions. Assume a reaction mixture passes at a volume rate of flow u (e.g., in m³/s), consider an element of volume $dV = Adx$ and one particular species component k , which enters this volume element at a concentration C_k , and leaves at $C_k + dC_k$ (in mol/m³). Here, A is the gas channel cross-section and dx is the distance traveled by the gas. If there is no longitudinal mixing, the net change with time of

the number of moles of k within dV , dn_k/dt , will be the sum of two terms: one due to chemical reaction within dV , and the other equal to the excess of species k entering dV over that leaving. Thus we have,

$$\frac{dn_k}{dt} = r_k dV - udC_k \quad (23)$$

The chemical reaction rate per unit volume is denoted by r_k . For H_2 fuel, we may write:

$$r_k dV = -\frac{I ds}{nF} = -\frac{Ia}{nF} dx \quad (24)$$

where a is the fuel channel width and I the current density. The $n = 2$ for H_2 and $n = 4$ for O_2 and $n = -2$ for H_2O as H_2O is created by the EC reaction. For a stable species concentration, $dn_k/dt = 0$, we have:

$$-\frac{Ia}{nF} dx = udC_k \quad (25)$$

or

$$C_k = C_{k0} - \int_0^x \frac{Ia}{unF} dx \quad (26)$$

The partial pressure can be calculated as:

$$P_k = C_k RT = P_k^0 - \Delta P_k \quad (27)$$

with

$$\Delta P_k = \int_0^x \frac{IaRT}{unF} dx \quad (28)$$

The total fuel and air pressures are obtained by the summations over the respective species partial pressures. For H_2 fuel, if current production is I , the rate of H_2 mole consumption is simply $dn_{H_2}/dt = -I/(2F)$, or

$$\frac{dP_{H_2}}{dt} = -\frac{IRT}{2Fu} \quad (29a)$$

For H_2 and CO fuel, we have:

$$\frac{d[P_{H_2} + P_{CO}]}{dt} = -\frac{IRT}{2Fu} \quad (29b)$$

The shift reaction described above can be used to determine dP_{H_2}/dt and dP_{CO}/dt . For fuel with CH_4 , we have:

$$\frac{d[P_{H_2} + P_{CO} + 4P_{CH_4}]}{dt} = -\frac{IRT}{2Fu} \quad (29c)$$

Together with the equilibrium composition determination described above, the respective component changes can be determined. Once the species concentrations or partial pressures are known at the gas inlet, the above equations give the variations of gas compositions and partial pressures in the gas channels when the temperature and current density distribution are given.

Notice that the x direction is the flow direction. Other than co-flow configuration, the air and fuel flows have different directions. By properly accounting for the flow directions, all co-, counter- and cross-flow designs can be treated.

In addition to the concentration and pressure changes described above, the pressure drop of the fuel flow through the channel due to viscosity (assuming laminar flow) is estimated by:

$$\Delta P = \frac{(1/2)\rho v^2 fl}{(Re D_h)} \quad (30)$$

where Re is the D_h -based Reynolds number, D_h the hydraulic diameter, l the length of the flow path, and f depends on the shape of the cross section of the channel, e.g., $f = 56.8$ and 64 for a square and a round channel, respectively [12]. Such simplification has been used to significantly reduce the computation cost [13].

2.5. Heat of reaction

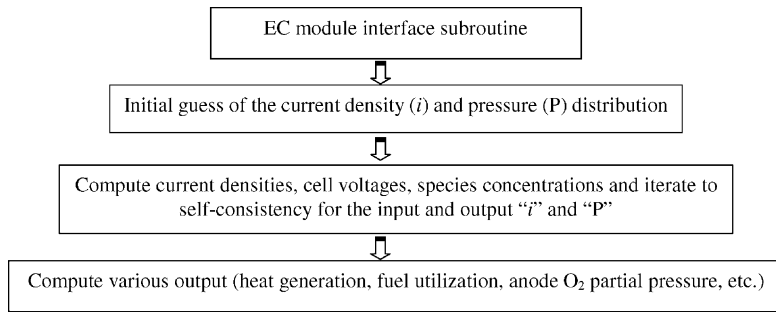
If one is interested in calculating the heat of chemical reaction due to composition change, the heat of reaction is simply the difference between initial system heat content (enthalpy) and the final system heat content. If one is concerned with EC reaction, then the heat content of O_2 needs to be included in the calculation of heat content change. The total heat production is the heat content decrease minus the delivered external electrical power, $H_i - H_f - V_{op}^* q$, where q is the charge involved (product of current and time) and V_{op} the fuel cell operating voltage. $H_i - H_f - V_{op}^* q$ is sufficient for a 2D description, which is one option of the EC module. For 3D models, additional details are the following: $H_i - H_f - q^* V_{th}$ is the chemical reaction heat and thermal irreversibility heat, where V_{th} is the Nernst potential, and can be viewed as heat released in the fuel channels and anode. $q^*(V_{th} - V_{op})$ is the total polarization (Ohmic, transport, activation) heat and released in the respective regions in accordance with polarization loss. In other words, the overall effective ‘‘Ohmic’’ resistance of the cell is:

$$\begin{aligned} R(i) &= \frac{E_{open} - V(i)}{i} \\ &= Ri + \left\{ b \sinh^{-1} \left(\frac{i}{2i_0} \right) - \left(\frac{RT}{4F} \right) \ln \left(\frac{1-i}{i_{O_2}} \right) \right. \\ &\quad \left. - \left(\frac{RT}{2F} \right) \ln \left(\frac{1-i}{i_{H_2}} \right) + \left(\frac{RT}{2F} \right) \ln \left(\frac{1 + p_{H_2}^0 i}{p_{H_2O}^0 i_{H_2}} \right) \right\} \end{aligned} \quad (31)$$

The total heat generated is $i^2 R(i)$. Heat generated by each R_i component can be reasonably assumed to be released to each respective component. For example, heat from i_{O_2} -term is released in cathode, and heat generated by i_{H_2} and i_{H_2O} terms are released in the anode. Heat from b -term is assumed to be released mainly in the cathode as the activation polarization is dominated by the cathode process. Therefore, most activation heat should be released in cathode, mainly in the reaction zone (about $10 \mu m$ thick) at the cathode–electrolyte interface.

3. The EC module and the linkage with MARC®

The EC module for the fuel cell modeling was programmed in a stand-alone code using FORTRAN 77 and can be executed if temperature field and the inlet flow information are available. The module is arranged as a single user-defined function (UDF) for interaction with external software. The main program structure can be seen as the following:



The EC code functions in several modes. These include:

- For a given operating voltage of a cell plate, the model computes the current density distribution according to the given uniform cell voltage.
- For a given total current, the model finds the cell operating voltage so that the integration of the local current density with the operating voltage yields the required total current.
- For a stack operation and given total voltage, the model determines each individual cell voltage so that they sum to the desired total voltage and the total current is the same for each individual cell.

3.1. The I – V sub-model

One function of the UDF is to calculate current density, cell voltage, and heat production in an SOFC stack, taking as inputs local values of the gas partial pressures and temperatures. The details of I – V relation and parameters therein have been described above. For recap, the cell potential, $V(J)$, for a given current density, given also the local values of the temperatures and gas partial pressures, is determined by the chosen I – V relation. It has the following characteristics:

- (a) Temperature and geometry dependence of Ohmic electrical resistance is considered explicitly. One is free to adjust the thickness of each individual cell component.
- (b) Temperature dependences of non-Ohmic overpotential terms by interpolations, aided by a few experimental data.
- (c) Partial pressure and geometry dependences of the non-Ohmic terms are included according to microscopic theory.

The UDF also computes the current density for a specified voltage. The current density is obtained by bisection search method. The initial current density range is between zero and the smaller of cathode and anode limiting current (less a small quantity, 10^{-6} , to avoid the logarithmic singularity). The implementation of several parameters and two forms of I – V curves allows for the code to be calibrated easily to available data taken from SOFC testing. The user can also create other desired I – V formula.

3.2. Grid

To adequately describe the local distribution of current density, heat generation, and species concentrations, a 3D grid is generated for a fuel cell(s) in a stack:

- (a) In the plan of the cell plate, a rectangular mesh is used for the EC active area. The grid points (x, y) , across the PEN structure, z , are associated pair-wise. Tests show one grid point for each $(1 \text{ cm} \times 1 \text{ cm})$ area gives adequate EC results, while one point for each $(0.5 \text{ cm} \times 0.5 \text{ cm})$ area provides practically convergent results.
- (b) For a set (x, y) in a cell, current is constant over the z -grid. The I – V relation is used to compute cell voltage if total current density is given or to find the current density consistent with a given cell voltage.
- (c) All cells in the stack have the same grid, but corresponding grid points in different cells can have different current densities.
- (d) Distributed heat productions are determined over the grids for the various terms in the I – V relation according to their respective physical origins.
- (e) As fuel cells are much thinner than the cell plate dimension, very few z points are required to obtain satisfying results. In fact, one can also choose to use a 2D grid, i.e., one z point for each PEN structure.

3.3. Cell voltage for a required total current

When the total current through a cell has been specified, the potential across the cell is determined according to the equipotential condition and resulting current density distribution integrated to the specified total current. The search is done by bisection with an initial range of between zero and the open circuit voltage.

- (a) The search for current for a voltage in the I - V submodel described above is used as a subset. The search is done for every (x, y) node.
- (b) Current at each node is integrated and compared to the specified total current. The search continues until convergence is achieved.
- (c) The search for each (x, y) node is independent of the others, and the total cost is linear to the number of (x, y) nodes. Cost of integration (step b) above is also linear to the number of (x, y) nodes. Therefore, the total cost is linear to the number of (x, y) nodes.

3.4. Self-consistence for the current generation and concentration distribution

The existing I - V subroutines require temperature profile and gas pressure distributions in the channels as input to find the desired I or V . In practice, only gas partial pressures in the gas inlets are known working parameters. The variation of partial pressures inside the channels is determined by the current density distribution, as shown in the subsection of the flow model (Fig. 1). Therefore, there is a coupled process between the current distribution and gas pressure distributions. A self-consistent determination of the gas pressures is required. This is done in the code by:

- (a) An initial guess of the current density distribution is generated by the overall operating conditions (e.g., inlet fuel pressures, working temperatures, cell voltage, or total current).
- (b) The current density distribution is used to find the gas pressure changes in the channels, as shown in the flow model.
- (c) The resulting gas pressures are used to determine the new current density.

- (d) The new current density distribution is mixed with the old current density to get the revised guess current density distribution.
- (e) Compare the total current, if operating voltage is set, or the operating voltage, if the total current is specified, and iterating until the self-consistent convergence is achieved.

3.5. Stack operation

- (a) When the total current through a stack of cells is specified, individual cell potential is determined separately and their sum gives the total output voltage. Each individual cell is independent of the others. The CPU requirement is linear to the number of cells in the stack.
- (b) If the total voltage is to be specified for a stack, all the cell voltages are adjusted such that their sum is the specified value while the total current is the same for each cell. As total current should be invariant for all the cells, it is used as the searching variable (i.e., case (a) is used as a subset). The cost is again linear to the number of cells in the stack. Typically, case (b) requires 10–20 times more CPU time than case (a).

The above is done self-consistently and the resulting current distribution, heat productions and cell voltages are all returned to the user.

3.6. EC module summary

We have described the theory and implementation details of an EC model capable of computing the current density distribution, chemical and electrical heat generation, and fuel cell efficiency. The EC model can address the dependence of fuel cell performance on the operating tempera-

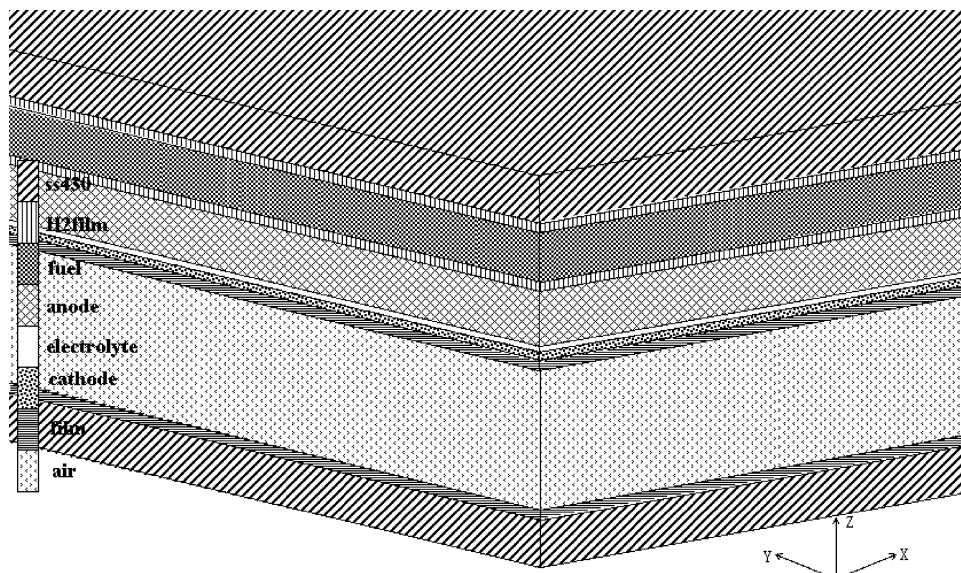


Fig. 1. MARC[®] model showing different materials through the thickness.

ture, fuel composition, gas pressure, flow rate, and geometry/configuration. The module can be linked easily to other simulation software to improve modeling quality, e.g., providing the FEA code with EC heat flux to facilitate thermal stress analysis, or assisting CFD with heat term and gas composition change.

3.7. Linking the EC module to MARC®

The basic procedure for the FEA–EC integration was to develop intermediary subroutines that will pass the cell temperature distribution to the EC subroutine and return the heat generation to MARC®. This is accomplished with a FLUX subroutine and it is supported by the use of state variables. State variables are used to track the composition of the gases; H₂, H₂O, CO, CO₂ and CH₄ in the fuel, and N₂ and O₂ in the air. Additional state variables track the heat generation and current density, which can be plotted subsequently through the plotting subroutine. The interface can be viewed simply as

MARC source subroutine (**flux**(f,ts,n,time))

Input temperature profile and geometry info↓ ↑return heat flux and other state variables

EC module interface subroutine

The EC subroutine is self-consistent and solves the entire mesh in one pass. The FLUX subroutine is called at every integration point for every element in the PEN. This discrepancy was accommodated by executing the EC subroutine from FLUX only once at the first integration point of the first element and placing the results in an array. Subsequent calls to FLUX then simply read the appropriate value stored in the array.

To use the MARC®–EC package, one is required to provide the necessary information such as the SOFC geometry, material properties, boundary conditions, operation parameters (e.g., fuel–air flow, working temperature, etc.). Such information can in principle be given through the MARC® graphical interface. It can also be specified in a procedure file. These procedures are common in using MARC®, and readers are referred to the MARC® documentation for details.

4. Sample results

As an example, a simple one-cell model is shown in Fig. 1. The model uses 11 elements through the thickness of the cell with the following 11 layers: two interconnect layers (SS430), two fuel film layers, two air film layers, one fuel layer, one air layer, one cathode layer, one electrolyte layer and one anode layer. The fuel and air are represented by three elements each. Thinner elements, designated as film elements, are located between the fluid and the solid elements. The thermal conductivity of these elements is adjusted so

that the heat conduction is equivalent to the actual convective heat transfer. The anode, electrolyte, and cathode are each modeled with a single element. Elements representing the interconnect are located at the top and bottom of the stack. Some of the material properties and cell component dimensions are shown in Table 1. Other parameters include the film coefficient: $h_{air} = 102.3 \text{ J/(s K)}$; $h_{H_2} = 1530 \text{ J/(s K)}$; corresponding to an equivalent conductivity of film layer = $h(\text{film coefficient}) \times t(\text{film layer thickness})$. Heat transfer mechanisms considered are convection and conduction. The model uses a 10×10 mesh of elements to represent the in-plane dimensions of the cell, which is an $11 \text{ cm} \times 11 \text{ cm}$ square cell. For a multi-cell stack, one can build a similar procedure file by repeating the corresponding layers.

To illustrate the modeling capability of the MARC®–EC package, Fig. 2 shows the steady-state temperature profiles for three flow designs (co-, counter- and cross-flow) with H₂ + CO fuel. Comparing the results with two different fuel flow rate ($V_{fuel} = 0.055$ and 0.0275 l/s , respectively), one

can see the significant impact of flow rate on the temperature distribution (and, therefore, on the thermal stress).

The modeling capability of the MARC®–EC tool is not limited to the steady-state analysis. This modeling tool can also be used for the evaluation of the transition from startup to steady-state conditions. As an example, Fig. 3 shows some snapshots of a fuel cell from startup to steady-state transition. The fuel cell was initially at $T = 0^\circ\text{C}$. The fuel and air flow were at $T = 700^\circ\text{C}$ and with flow rate of, respectively, 0.0825 and 0.33 l/s . The fuel cell was set at a working voltage of $V = 0.7 \text{ V}$ when it is warm enough to have current production.

Due to the nature of the MARC® FEA method, the numerical results are very stable. The entire comparable transient results are almost identical for time steps ranging from 0.2 to 12 s —a significant advantage over a typical CFD algorithm. The startup modeling has demonstrated that startup will not occur in an isothermal manner. Steady-state operating conditions will result in a different temperature distribution due to the heat transfer and fuel consumption along the length of the cell. The startup procedure and steady-state conditions will each need to be controlled to maintain an adequate safety factor below the material failure points. In the same manner, however, starting the EC reaction after the cell is heated also needs to be carefully controlled. This tool can be used to identify and prevent conditions where localized thermal runaway may occur. Similarly, any disturbance to steady-state operating conditions can be evaluated.

As another example, Fig. 4 shows the cell voltage variation for a 30-cell stack ($V_{tot} = 21 \text{ V}$) at the steady state.

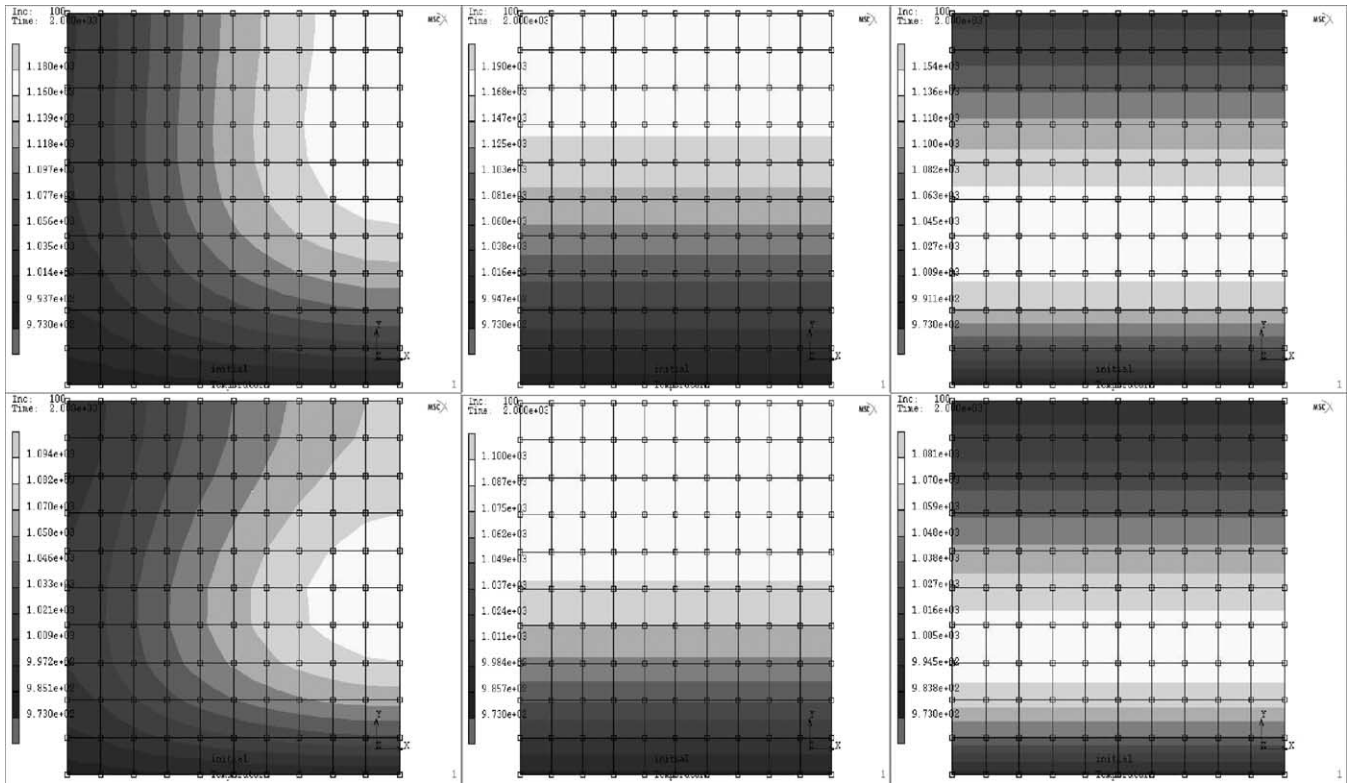


Fig. 2. Temperature profiles of cross-, co- and counter-flow designs. Upper row: $V_{fuel} = 0.055$ l/s; lower row: $V_{fuel} = 0.0275$ l/s.

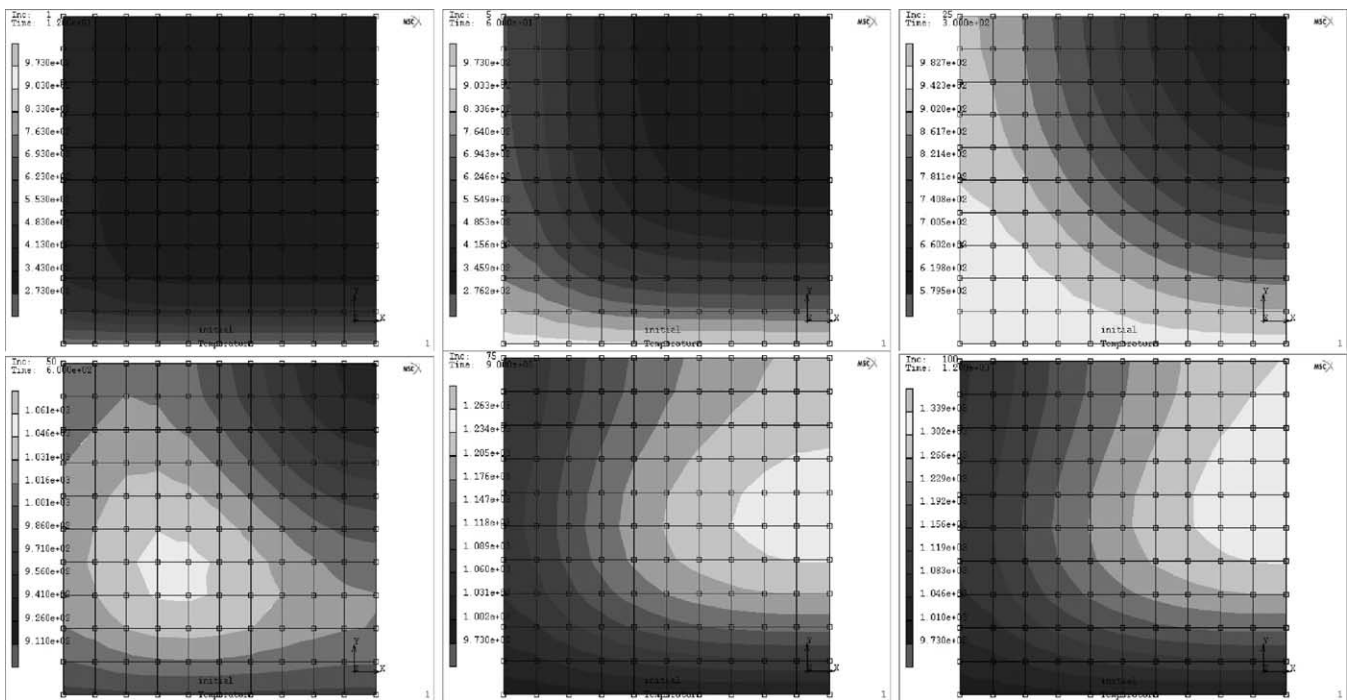


Fig. 3. Snapshot of the transition from start-up to steady-state conditions. Shown are for start-up time, t : (a) 12 s, (b) 60 s, (c) 300 s, (d) 600 s, (e) 900 s, (f) 1200 s.

Table 1
Some material and geometry parameters used in the simulation

	Thickness (m)	Heat conductivity (J/m K s)	Specific heat capacity (J/kg K)	Mass density (kg/m ³)
Interconnect layer	5e-4	25.5	800	7700
Air film layer	1e-4	102.3e-4	100	0.3236
Air layer	1.5e-3	0.0692	1156	0.3236
Cathode	5e-5	2.5	520	6350
Electrolyte	1e-5	2	460	6010
Anode	6e-4	22.5	466	4200
Fuel film layer	1e-4	1530e-4	100	0.0224
Fuel layer	5e-4	0.450	15156	0.0224

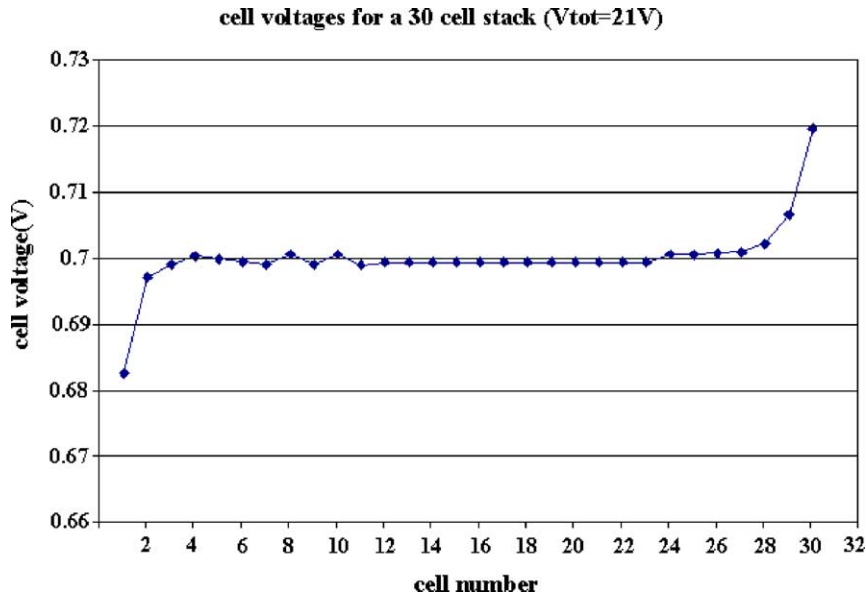


Fig. 4. The cell voltage variation of a 30-cell stack ($V_{tot} = 21 V$) at the steady state.

As can be seen, only the outmost top and bottom 2–3 cells deviate substantially from the average cell voltage. Similar results are found for 8- and 15-cell stacks.

Numerical characteristics of the MARC[®]-EC tool can be seen in Tables 2 and 3 (performed on one SGI RISC14000 processor, 400 MHz). The CPU time requirement increases roughly linearly with the number of cells in the stacks. Typically 20–40 increments are needed for a steady-state run. Therefore, one can get the steady-state results for a 30-cell stack in a few minutes if the total current is the desired criteria. Even if the total stack voltage is the control criteria, the results can be obtained in a few hours of CPU time in a

Table 2
CPU time when specifying total current or fuel utilization

No. of cells	Time/inc (s)
2	0.45
3	0.68
4	0.91
5	1.15
8	1.83
15	3.48
30	6.93

Table 3
CPU time when specifying total voltage

No. of cells	Time/inc (s)
2	14.0
3	26.8
4	36.3
5	51.8
8	53.0
15	149
30	326

single process. Consequently, one can examine various stack designs readily with this tool.

5. Summary

We have described the technical details of a multi-physics computational tool for SOFC modeling, the MARC[®]-EC package. The description focuses on the development of an electrochemistry module to supplement the capability of MARC[®] to model SOFCs. Numerical results are given to demonstrate the modeling capability and numerical

efficiency of the tool. The tool can be used to perform parametric studies that are important to system designs. The MARC[®]-EC package offers significant advantages in terms of numerical stability and computational efficiency over that of a CFD code such as STAR-CD or Fluent.

Acknowledgements

The work summarized in this paper was funded as part of the Solid-State Energy Conversion Alliance (SECA) Core Technology Program by the US Department of Energy's National Energy Technology Laboratory (NETL). PNNL is operated by Battelle for the US Department of Energy under Contract DE-AC06-76RL01830.

References

- [1] K. Recknagle, R. Williford, L. Chick, D. Rector, M. Khaleel, J. Power Sources 113 (2003) 109.
- [2] J. Kim, A. Virkar, K. Fung, K. Metha, S. Singhal, J. Electrochem. Soc. 69 (1999) 146.
- [3] W.J. Moore, Physical Chemistry, 3rd ed., Prentice-Hall, Englewood Cliffs, NJ, 1962.
- [4] N. Minh, Chemtech. (February 1991) 120.
- [5] J.A.M. Van Roosmalen, E.H.P. Cordfunke, Solid State Ion. 52 (1992) 303.
- [6] L.A. Chick, J.W. Stevenson, K.D. Meinhardt, S.P. Simner, J.E. Jaffe, Modeling and Performance of Anode-Supported SOFC, in: Proceedings of the Fuel Cell 2000 Seminar, Pacific Northwest National Laboratory, Richland, WA.
- [7] Fuel Cell Handbook, 5th edition, EG&G Services, Parsons, Inc., Sciences Applications International Corporation, October 2000.
- [8] E.N. Fuller, P.D. Schettler, J.C. Giddings, Ind. Eng. Chem. 19 (1966) 58.
- [9] E.P. Murray, T. Tsai, S.A. Barnett, Nature 649 (1999) 400.
- [10] S. Park, J.M. Vohs, R.J. Gorte, Nature 404 (2000) 265.
- [11] E.L. Cussler, Diffusion: Mass Transfer in Fluid Systems, Cambridge University, Cambridge, 1984, Chapter 8.
- [12] R.J. Boersma, N.M. Sammes, Computational analysis of the gas-flow distribution in solid oxide fuel cell stacks, J. Power Sources 63 (1996) 215–219.
- [13] E. Achenbach, U. Reus, The effect of mass flow distribution on the characteristics of a solid oxide fuel cell system, Electrochem. Soc. Proc. 99 (19) (1999) 1125–1134.